PREPRINT. Accepted for publication, Physics of Plasmas

High-Gain Direct-Drive Target Design For Laser Fusion

S. E. Bodner[1*], D. G. Colombant, A. J. Schmitt, and M. Klapisch[2]
Plasma Physics Division, Naval Research Laboratory, Washington, DC 20375
1. Current address: 689 Fearrington Post, Pittsboro, NC 27312
2. ARTEP Inc, Columbia, MD 20145

Abstract
A new laser fusion target concept is presented with a predicted energy gain of 125 using a 1.3 MJ KrF laser. This energy gain is sufficiently high for an economically attractive fusion reactor. X-rays from high- and low-Z materials are used in combination with a low-opacity ablator to spatially tune the isentrope, thereby providing both high fuel compression and a reduction of the ablative Rayleigh-Taylor instability.

PACS numbers: 52.58.Ns, 52.25.Nr, 52.35.Py, 52.75.-d

A laser fusion power plant will probably require energy gains from the target of more than 100 to overcome the low efficiency of the laser. For example, the Sombrero reactor study[1] assumed an energy gain of 114, using a 7.5% efficient 3.4 MJ krypton-fluoride (KrF) laser. Unfortunately it has been difficult to design a laser fusion target with these high energy gains that is at the same time consistent with the physics constraints of controlling hydrodynamic instabilities. We have now developed a target design with a predicted energy gain of 125 using a 1.3 MJ KrF laser, and preliminary analysis indicates that it is consistent with the currently-understood constraints from the ablative Rayleigh-Taylor instability. Gains would be even higher with more laser energy.

The highest possible coupling efficiency from a laser to a spherically imploding DT fuel utilizes the "direct-drive" concept, in which multiple laser beams directly and symmetrically illuminate the spherical target. As an example, the predicted laser absorption efficiency for our target design is 89%, and the predicted rocket implosion efficiency is 10%. The net coupling efficiency of 8.9% (from incoming laser energy to imploding DT kinetic energy) compares very favorably with the "indirect-drive" ignition target design[2] for the National Ignition Facility which has a predicted net coupling of less than 1.5%.

In 1995 scientists at the Naval Research Laboratory (NRL) completed a few-kilojoule KrF gas laser called Nike, and demonstrated that it could produce ultra-uniform laser illumination[3] using an optical smoothing technique that induces spatial and temporal incoherence in the laser beams. Each laser beam, at 1 THz bandwidth, has a measured time-averaged intensity nonuniformity at the focal plane of only 1% rms (excluding tilt and curvature). With multiple beam overlap, the laser nonuniformity drops to approximately 0.2% rms (excluding the higher-mode interference between the laser beams). In the succeeding years[4] Nike has been used to ablatively accelerate plastic foils on a low isentrope by using a pulse with a low intensity foot. With Nike's high quality illumination, the mass nonuniformity generated by the laser imprint during the foot of the pulse was observed to be very small, equivalent to less than 100 Å rms surface nonuniformity. In a spherical high-gain implosion the imprinted mass perturbations would differ because of the different target materials, laser geometry, and laser pulse duration, but Nike's low mass imprinting is nonetheless very encouraging.

Since the compressed shell is being accelerated inward by a lower-density plasma corona, the ablation interface between the two regions is unstable to the Rayleigh-Taylor (RT) fluid instability. This instability can be ameliorated[5] by preheating the target, thereby reducing its density. The reduced density leads to an increase in the mass ablation velocity, and this velocity flow then convects the RT instability away from the ablation surface. A previous target design[6] proposed using an all-DT target and preheating it with an enhanced shock wave, but the shock raised the isentrope of both the ablator and the fuel. The increase in the fuel isentrope then led to a reduced spark-plug compression and a reduced energy gain. There appeared to be a basic conflict between the requirement to preheat the ablator and the requirement to not preheat the main fuel region.

Recently we suggested [Ref. 6] that one way of resolving this conflict would be to spatially tune the target isentrope with x-rays instead of shocks, thereby putting part of the ablator on a higher isentrope than the main DT fuel. This proposal has now been developed into the design and calculations of a specific target to be presented here, and illustrated in

Fig. 1a. The DT fuel is surrounded by an ablator that is a CH foam (~ 10 mg/cm^3) filled with frozen DT; the ablator can be written chemically as $CH(DT)_{64}$. The ablator is surrounded by a thin plastic shell to confine the DT, and then by a thinner high-Z overcoating such as gold.

The $CH(DT)_{64}$ ablator, mostly hydrogen isotopes, provides the low opacity that is needed for penetration by soft x-rays. During the first few nanoseconds of the laser pulse, the gold overcoat heats to ~ 70 eV, producing broadband x-radiation that penetrates into the ablator below the K-edge of cold carbon which is at 285 eV. The gold is blown far from the target during the foot of the pulse and does not produce significant x-radiation after ~ 10 ns. We found that 300–350 Å of gold was needed for significant ablator preheating and RT reduction; a 200 Å overcoat produced negligible ablator preheat; a 400 Å overcoating produced enough x-rays to heat through to the fuel layer and prevent ignition. In addition to x-ray preheating, the gold increases the early-time separation between the absorption and ablation surfaces from ≤ 10 μm to ~ 200 μm. This separation should relax the requirements on the laser uniformity. The gold has the side benefit of increasing the infrared albedo of the target during its injection into the reactor chamber.

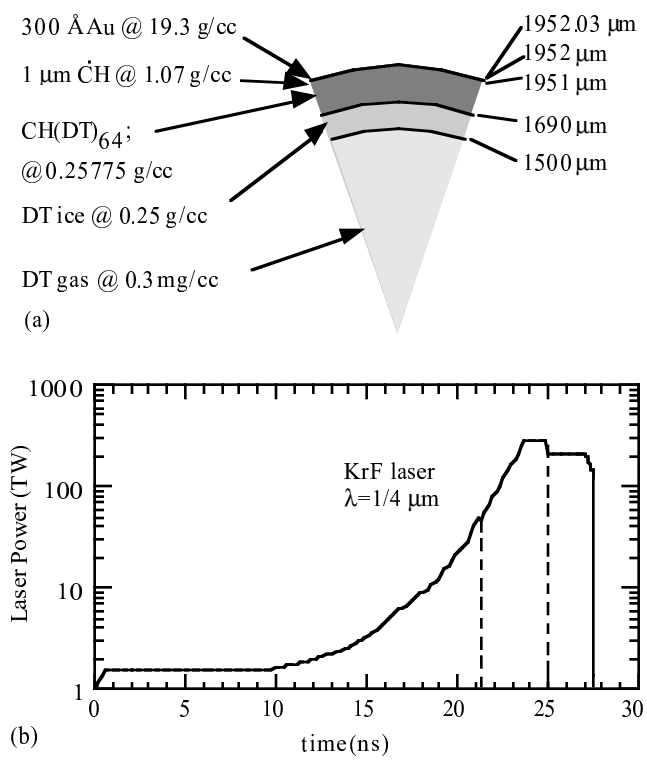

Fig. 1 (a) High gain direct-drive target parameters using a 1.3 MJ KrF laser. The ablator is a CH foam at ~ 10 mg/cm^3 filled with frozen DT. (b) Laser pulse shape. The dashed lines at 21.2 ns and 25 ns indicate when the laser beam is zoomed inward; i.e., it is reduced in size to match the imploding target.

The laser pulse shape is shown in Fig. 1b. To enhance the laser-target coupling efficiency we utilized an important concept[7] called "zooming": the laser's focal diameter was reduced in size to follow the target inward, first to 74% and then to 54% of the initial spot diameter. This zooming is conceptually easy to achieve with the beam smoothing technique used on a KrF laser such as Nike, because the intensity distribution at the target is an image of an aperture located at the low energy stage in the laser. Zooming is achieved by using multiple apertures, with the image of the largest aperture relayed first, followed by successfully smaller apertures. Electro-optic techniques may eventually provide continuous zooming. Zooming reduces the laser energy requirement for this target from 2.1 MJ to 1.3 MJ, and raises the predicted gain from 72 to 125. (Shock breakout at the inner surface, and the inward acceleration, begin at 20.5 ns. The shell implosion velocity reaches 3.4×10^7 cm/s. The average acceleration inward during the main laser pulse is 5.74×10^{15} cm/s^2. Bang time is 28.17 ns. The hot spot ignition radius is 60 μm at an average density of 62 g/cm^3. The maximum fuel density reaches 560 g/cm^3, and the total ρR of the target is 1.8 g/cm^2. The predicted yield is 160 MJ.)

FAST1D (the spherical one-dimensional computer model used in the above study) solves the mass, momentum, and energy fluid equations using the FCT (Flux Corrected Transport) formalism, with a sliding-zone Eulerian mesh that provides good resolution in the physically important regions[8]. Laser transport and absorption use ray tracing and inverse bremsstrahlung. Multigroup diffusion models are used for both radiation and alpha particle transport. Electron and ion heat conduction use the Spitzer form with flux limiting. Tabular lookups are used for real material equation-of-state and radiation opacity. The STA model is used to generate tabular LTE Planck and Rosseland opacities, and then the Busquet algorithm is used[9] to modify the data base for non-LTE radiation physics. Typically we use 45 radiation groups, non-evenly distributed; the groups are chosen to resolve the dominant emission and absorption energy lines and the continuum.

Figure 2 shows contours of constant isentrope during the implosion. The isentrope is approximated here by a pressure ratio defined as $\alpha = (P_e + P_i)/P_{FD}$, where P_e and P_i are the electron and ion pressure, and P_{FD} is the Fermi-degenerate electron pressure of fully ionized material. (It is assumed that the DT and the CH foam have been uniformly mixed.) Fig. 2 shows that the $CH(DT)_{64}$ ablator is preheated by the soft gold radiation during the first 10 ns of the laser pulse, and then by the carbon radiation during the high

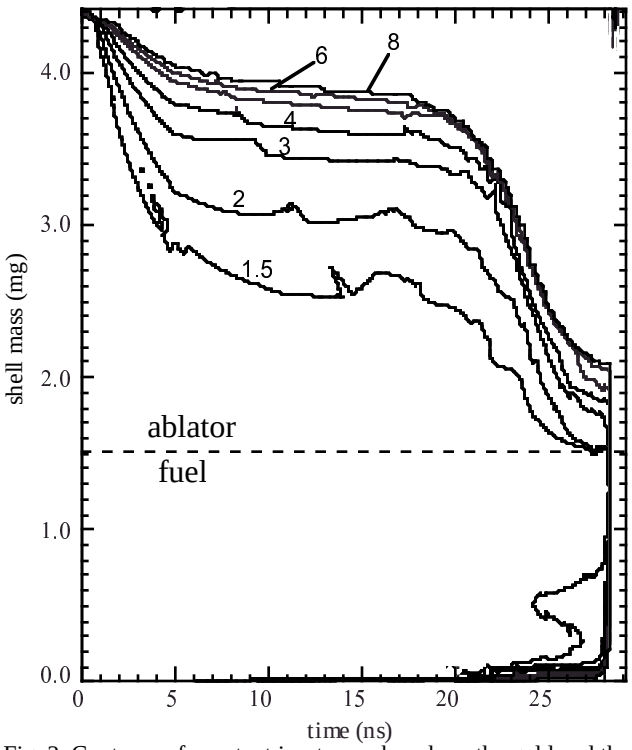

Fig. 2 Contours of constant isentrope show how the gold and the carbon radiatively preheat the ablator material. The main fuel stays near the minimum Fermi-degenerate isentrope. The ordinate is the integrated shell mass from the center of the target.

intensity portion of the laser pulse. The pure DT fuel stays on a very low isentrope, with $\alpha \sim 1.0$.

We had originally designed the target to rely solely upon gold x-rays to heat the ablator. However parameter studies in which we varied the carbon density and gold thickness show that there is also significant heating of the target by carbon x-rays, and the optimal preheating uses a combination of these two sources. There is about a factor of two flexibility in the choice of the CH foam density: above ~ 20 mg/cm^3 there is significantly less x-ray preheating; below ~ 5 mg/cm^3 the x-rays penetrate to the inner edge of the ablator which then thermally preheats the main DT fuel. In the base case, with 10 mg/cm^3, the Attwood number at the ablator/fuel interface is less than 0.1 during most of the inward acceleration. Thus the RT at the ablator/fuel interface (a separate instability) is probably not important for this target.

The laser fusion community has developed a variety of methods for assessing the ablative RT instability. The simplest guideline is the distance-moved-over-thickness, $DMOT = (R_0 - R)/\Delta R$, where R_0 is the initial outer radius of the target, $R(t)$ is the mass-averaged shell radius, and $\Delta R(t)$ is shell thickness measured to the 1/e values from the peak density. *DMOT* is proportional to $\int\sqrt{kg}\,dt$, the number of classical e-folds of the RT instability, for a perturbation wavelength $1/k$ that is comparable to the shell thickness. Another commonly-used parameter is the in-flight-aspect-ratio, $IFAR = R/\Delta R$ which is closely related to $\int\sqrt{kg}\,dt$. These two parameters are plotted in Fig. 3. At 24 ns, near the time of peak inward acceleration, the *DMOT* reaches 40 and the peak *IFAR* reaches 60. These values then decrease as ΔR thickens due to radial convergence. Whether the values are acceptable for direct-drive targets depends in practice upon the level of nonuniformities in the laser and in the target fabrication.

The next level of accuracy and complexity uses a dispersion relation for the RT growth. We used the formula, $\gamma = \sqrt{kg/(1+kL)} - 3k(dm/dt)/\rho_{\max}$, where g is the inward acceleration, L is the shortest density scale length at the ablation front, $k = \ell/R(t)$ where ℓ is the mode number, and $(dm/dt)/\rho_{\max}$ is the mass ablation velocity at the peak density. Weber et al[10] found that the above formula is a good fit to their hydrodynamic computer simulations. Since the main topic of this article is the ablative RT instability, we specified the mass inhomogeneity at 20 ns, the beginning of the inward acceleration phase. For a mode spectrum, including both laser imprinting and fabrication, we assumed that the rms amplitude of the perturbation in Angstroms is given by:

$$A(t) = \sqrt{\sum_{\ell}(2\ell+1)\left(A_\ell\,\ell^{-5/4}\right)^2}$$

where $\ell = 2^n, n = 1,\ldots,11$. Following the suggestion of Haan[11], all modes within a factor of two have been combined coherently and considered as a single mode. Modes farther apart are assumed to have independent phases. The A_ℓ are chosen to be equal at 20 ns, with their weighted rms sum $A(t{=}20) = 500$ Å. Each of the A_ℓ then grow according to the above RT dispersion relation. Figure 4 shows $A(t)/\Delta R(t)$, for the case of $A(t{=}20) = 500$ Å. The ratio only reaches 18% at 26.5 ns, near the peak inward acceleration, with 5.8 e-folds of growth. We conclude that our target may survive the RT instability, if the total perturbation

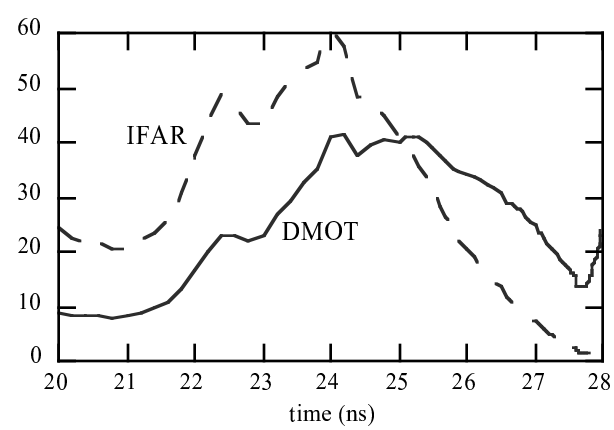

Fig. 3 In-flight-aspect-ratio (IFAR) and distance-moved-over-thickness (DMOT) during the shell's acceleration inward. They reach a maximum near the peak acceleration inward.

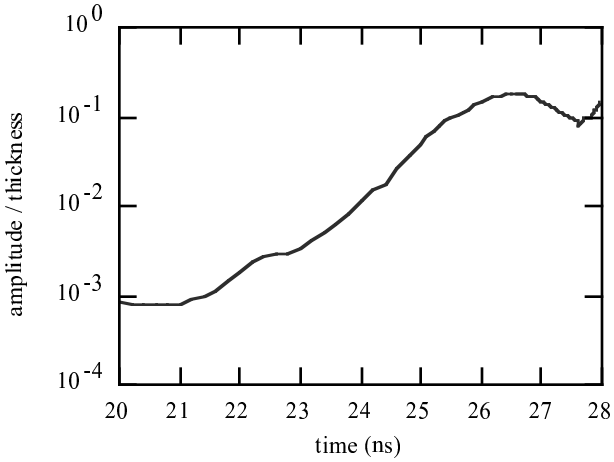

Fig. 4 The ratio of the rms amplitude of the shell perturbation to the shell thickness, versus time, using a model dispersion relation for the Rayleigh-Taylor instability. The amplitude is predicted to remain less than the shell thickness if the initial perturbation is less than 500 Å.

amplitude is less than 500 Å at the end of the foot of the laser pulse, and if the initial mode spectrum and RT growth rate formulas are in the final analysis similar to what we have assumed. (The results in Fig. 4 also contain a model [11] to evaluate the effects of saturation, but the predicted perturbation amplitudes are low enough so that the saturation effects are not important.)

We also considered two other dispersion relations for the growth rate γ: the curve-fit formula of Takabe[12] in which $L \to 0$ and there is a factor of 0.9 in front of the square root; and the analytically derived and more complex formula of Sanz[13]. The Sanz formula gave the largest *A(t)/ΔR(t)* (38%) and the Takabe relation the lowest (10%). There are of course basic physics limitations in all of these dispersion relations, so we can only conclude that there is some reasonable possibility that our target design concept will survive the ablative RT instability, if the imprint in the foot of the pulse can be held to ~ 500Å.

The next level of accuracy and complexity would be a 2D (two-dimensional) arbitrary-Lagrangian-Eulerian code, or an adaptive-grid-Eulerian code. These codes can calculate the laser imprinting in the foot of the laser pulse, follow the RT instability into the late-time nonlinear regime, and include the multi-mode incoherent laser illumination. We have such an adaptive-grid Eulerian code at NRL called FAST2D [8]. An accurate resolution of a wide spectrum of modes is demanding in computer resources, especially when it includes a wide range of physics packages and accurate radiation transport. However the most difficult challenge has not been the late-time nonlinear evolution of the RT instability, but rather the simultaneous calculation of the early-time blowoff of a 300 *Å* thick gold layer and the ablative RT perturbations that has important wavelengths of hundreds of microns. NRL scientists hope to present some 2D computer analysis of this target design in the near future using the FAST2D code, but there are no results yet.

Using the short laser wavelength of 1/4 μm provides the maximum absorption efficiency and the maximum rocket implosion efficiency, along with the lowest risk of laser-plasma instabilities. A KrF laser at 1/4 μm also has the advantage of flexible zooming that enhances the coupling efficiency and gain. However there is some interest in the fusion community in the long-term potential of a 1/3 micron solid state laser. We have therefore taken the same target described in Fig. 1(a), and retuned it for 1/3 micron light, assuming the same two-step zooming. Zooming of individual laser beams is not practical for solid state lasers because they can not relay an image from the laser's front end, but in principle one could triple the number of laser beam lines, and use each third to produce different image sizes. The yield of the target with 1/3 μm and zooming was 155 MJ, nearly the same as with 1/4 μm. However the absorption and rocket efficiencies were sharply reduced, and the laser energy required to drive this target increased to 1.8 MJ. The energy gain thus dropped to 78. To compensate for this lower gain one would need a higher laser efficiency and a lower capital cost per Joule.

In this paper we have put forward for the first time a high gain target that may also provide sufficient control of the ablative RT hydrodynamic instability. Gains well above 100 are possible through the use of (a) direct-drive laser-target coupling; (b) controlled levels of radiative preheat in a low-opacity ablator, (c) a 1/4 μm laser wavelength, and (d) zooming so that the image size follows the target as it implodes. The ablative RT instability that we have addressed in this article is important during the implosion phase which begins at 20.5 ns, when the inside edge of the shell begins to accelerate inward. We are still evaluating the first 20.5 ns of the pulse, the so-called "imprint" phase, in which the laser nonuniformities induce Richtmyer-Meshkov modes and seed the ablative RT instability. As we noted above, the 2D computational analysis of this imprint phase is challenging because of widely differing scale lengths (a thin gold coating and long laser perturbation wavelengths). Our 2D codes also assume that the laser and target perturbations are in the form of stripes; a 3D simulation will eventually be needed to model the real laser speckle and RT instability.

We have not evaluated here the separate RT instability that occurs as the dense shell decelerates against the hot central ignitor. Because of density gradient stabilization, this deceleration instability is most important for mode numbers ≤ 10, and is

largely decoupled from the ablative instability which is most dangerous for mode numbers ~ 100. Our 2D implosion studies suggest that the deceleration RT is unimportant if one uses KrF lasers since they also have good beam uniformity in the low mode perturbations. The major uncertainty with the deceleration RT is whether one can obtain sufficiently accurate laser beam alignment and target fabrication sphericity. Our computations show another fluid instability[14], called the "radiating plasma structure", which can introduce deleterious density waves and preheating. Some evidence of this structure is visible in Fig. 2 as the notch in the α=1.5 isentrope at 14 ns. However by carefully tuning the laser pulse we were able to avoid the deleterious effects of this instability.

We also have not discussed the various laser-plasma instabilities. Preliminary analysis indicates that these instabilities are near threshold and may be tolerable because of the KrF laser's short 1/4 μm wavelength and the modest peak laser intensity ($<10^{15}$ W/cm^2), but more theory and experiment are required. We have also assumed that the CH foam and the DT in the ablator are uniformly mixed from the beginning of the acceleration phase. We have some preliminary experimental and computational evidence that this is not correct. We are assuming that the laser pulse shape can be retuned to correct for the actual shock velocities.

This work was supported by the U.S. Dept. of Energy under a contract to NRL. John Gardner provided important advice. One of the authors, S. B., initiated this research while an employee at NRL and completed it through a consulting contract with SAIC.

* Electronic address: a-s.bodner@mindspring.com

[1] I. V. Sviatoslavsky, M. E. Sawan, R. R. Peterson, G. L. Kulcinski, J. J. MacFarlane, L. J. Wittenberg, H. Y. Khater, E. A. Mogahed, S. C. Rutledge, Fusion Technol. **21**, 1470 (1992)

[2] J. Lindl, Phys. Plasmas, **2,** 3933 (1995)

[3] S. P. Obenschain, S. E. Bodner, D. Colombant, K. Gerber, R. H. Lehmberg, E. A. McLean, A. N. Mostovych, M. S. Pronko, C. J. Pawley, A. J. Schmitt, J. D. Sethian, V. Serlin, J. A. Stamper, C. A. Sullivan, J. P. Dahlburg, J. H. Gardner, Y. Chan, A. V. Deniz, J. Hardgrove, T. Lehecka, M. Klapisch, Phys. Plasmas **3**, 2098 (1996)

[4] C. J. Pawley, S. E. Bodner, J. P. Dahlburg, S. P. Obenschain, A. J. Schmitt, J. D. Sethian, C. A. Sullivan, J. H. Gardner, Y Aglitskiy, Y. Chan, T. Lehecka, Phys. Plasmas **6**, 565 (1999)

[5] S. E. Bodner, Phys. Rev. Lett., **33**, 761 (1974)

[6] S. E. Bodner, D. G. Colombant, J. H. Gardner, R. H. Lehmberg, S. P. Obenschain, L. Phillips, A. J. Schmitt, J. D. Sethian, R. L. McCrory, W. Seka, C. P. Verdon, J. P. Knauer, B. B. Afeyan, H. T. Powell, Phys. Plasmas **5**, 1901 (1998)

[7] R. H. Lehmberg and J. Goldhar, Fusion Technology 11, 532 (1987)

[8] J. H. Gardner, A. J. Schmitt, J. P. Dahlburg, C. J. Pawley, S. E. Bodner, S. P. Obenschain, V. Serlin, Y. Aglitskiy, Phys. Plasmas, **5**, 1935 (1998)

[9] M. Klapisch, A. Bar-Shalom, J. Oreg, and D. Colombant, Phys. Plasmas **5**, 1919 (1998)

[10] S. V. Weber, S. G. Glendinning, D. H. Kalantar, M. H. Key, B. A. Remington, J. E. Rothenberg, W. Wolfrum, C. P. Verdon, J. P. Knauer, Phys. Plasmas **4**, 1978 (1997)

[11] S. W. Haan, Phys. Fluids B **3**, 2349 (1991)

[12] H. Takabe, K. Mima, L. Montierth, and R. L. Morse, Phys. Fluids **28**, 3676 (1985)

[13] J. Sanz, Phys. Rev. E **53**, 4026 (1996)

[14] G. Hazak, A. L. Velikovich, M. Klapisch, A. J. Schmitt, J. P. Dahlburg, D. Colombant, J. H. Gardner, L. Phillips, Phys. Plasmas **6**, 4015 (1999)